Welcome to Today's Webinar!

MODELING PHOTODETECTORS USING THE DRIFT-DIFFUSION EQUATIONS FOR RF-PHOTONICS APPLICATIONS

15 July 2021 • 10:00 EDT (UTC -4:00)

OSA Photonic Detection Technical Group

Technical Group Executive Committee

Giuseppe D'Aguanno
Chair
Johns Hopkins University, Applied Physics Laboratory

Achyut Dutta
Vice Chair
Founder Banpil Photonics

Shuren Hu
Events Officer
SiLC Technology

Kimberly Reichel
Webinar Officer
3DEO, Inc.

Vivek Nagal
Social Media Officer
Johns Hopkins University

About the Photonic Detection Technical Group

Our technical group focuses on detection of photons as received from images, data links, and experimental spectroscopic studies to mention a few. Within its scope, it is involved in the design, fabrication, testing of single and arrayed detectors. Detector materials, structures, and readout circuitry needed to translate photons into electrical signals.

Our mission is to connect the 2000+ members of our community through technical events, webinars, networking events, and social media.

Our past activities have included:

- Special sessions at CLEO and OFC, including a panel discussion on *Silicon Photonics for LiDAR and Other Applications*
- 11 previous webinars

Connect with our Technical Group

Join our online community to stay up to date on our group's activities. You also can share your ideas for technical group events or let us know if you're interested in presenting your research.

Ways to connect with us:

- Our website at www.osa.org/pd
- On LinkedIn at https://www.linkedin.com/groups/8297763/
- Email us at TGactivities@osa.org

Today's Speaker

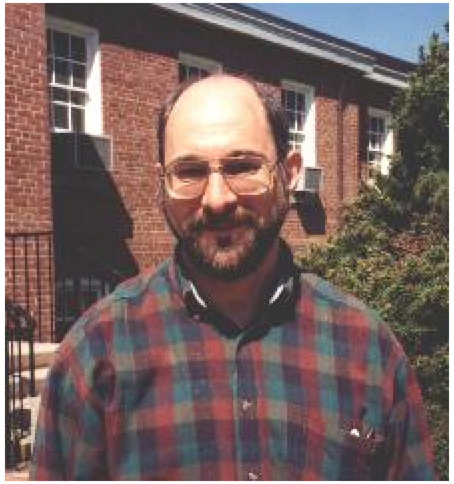

Curtis R. Menyuk

University of Maryland Baltimore County

Short Bio:

- Professor, University of Maryland Baltimore County (USA)
- Research Interests: Modeling of photonic systems
- APS Fellow, OSA Fellow, IEEE Fellow, IEEE Photonics Society William Streifer Award (2013), Humboldt Foundation Research Award (2015)

Modeling photodetectors (PDs) using the drift-diffusion equations for RF-photonics applications

Curtis R. Menyuk, Ehsan Jamali, Y. Hu, M. Hutchinson, J. D. McKinney, V. J. Urick, and K. J. Williams

July 15, 2020

UMBC

Table of contents

UMBC

What is a PD

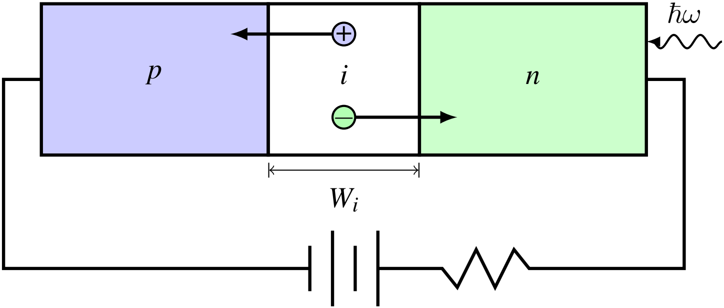

- Optical intensity is transferred to the electric current
- The bandwidth or response time is constrained by
  - transit time
  - RC time constant

Nonlinear distortion and noise limit the PD performance

UMBC

Motivation

- High-current, high-power PDs are important in
  - RF-photonic systems[1]
  - Optical communication systems[1]
  - Photonic microwave generation systems[2]
- Phase noise in PDs is a critical limiting factor in many RF-photonic applications[3]
- Device nonlinearity limits the performance of these PDs

[1] A. Seeds and K. Williams, J. Lightw. Technol. **24**, 4628–4641 (2006).
[2] T. M. Fortier et al., Opt. Lett. **38**, 1712–1714 (2013).
[3] V. J. Urick et al., *Fundamentals of Microwave Photonics* (Wiley, 2015).

UMBC

RF-photonic system

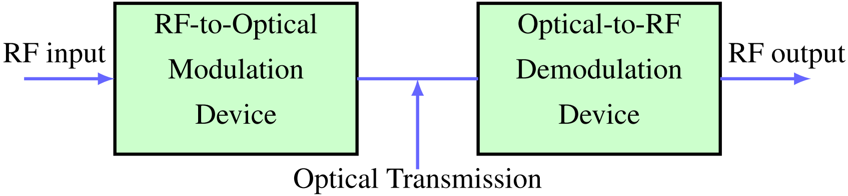

High-current, high-power PDs are important in

- RF-photonic systems
- optical communication systems

UMBC

RF-photonic system

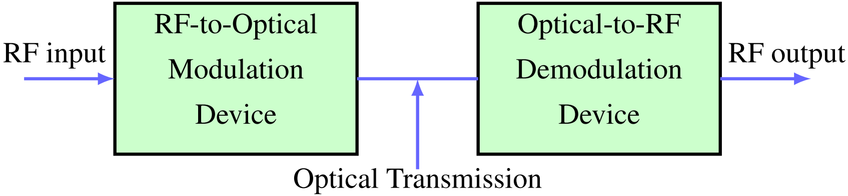

- RF-photonic systems have advantages over purely electronic systems[1]
  - low transmission loss
  - large bandwidth
  - reduced size
  - immunity to electromagnetic interference
- RF-photonic systems also have some drawbacks
  - low transmission power
  - nonlinear distortion
  - spurious free dynamic range (SFDR)

[1] A. Seeds and K. Williams, J. Lightw. Technol. **24**, 4628–4641 (2006).

UMBC

History

- In the mid-1990s, Williams et al. developed a 1D model of high-current PDs, based on the drift-diffusion equations[1]
- In 1997, Wilson and Walker developed 1D and 2D models of metal-semiconductor-metal PDs to study the transient behavior of the PDs[2]
- In 2000, Jiang et al. developed a circuit-equivalent model to study distortion in a *p-i-n* PD[3]

[1] K. J. Williams et al., J. Lightw. Technol. **14**, 84–96 (1996).
[2] S. P. Wilson and A. B. Walker, Semiconduct. Sci. Technol. **12**, 1265–1272 (1997).
[3] H. Jiang et al., IEEE Photon. Technol. Lett. **12**, 540–542 (2000).

History

- In 2011, Fu et al. used a 1D drift-diffusion model to study the nonlinear intermodulation distortion in a modified uni-traveling-carrier (MUTC) PD[1]
- In 2014, Hu et al. developed 1D and 2D drift-diffusion models to study sources of nonlinearity in a *p-i-n* PD[2]
- In 2017, Hu et al. developed a 1D drift-diffusion model to study amplitude-to-phase conversion in an MUTC PD[3]

[1] Y. Fu et al., IEEE J. Quantum Electron. **47**, 1312–1319 (2011).
[2] Y. Hu et al., J. Lightw. Technol. **32**, 3710–3720 (2014).
[3] Y. Hu et al., IEEE Photon. J. **9**, 5501111 (2017).

UMBC

History

- In 2019, Jamali et al. used a 1D drift-diffusion model to calculate phase noise in MUTC PDs[1]
- In 2020, Jamali et al. developed a model to study the impact of nonlinearity including bleaching in MUTC and *p*-*i*-*n* PDs on RF-modulated electro-optic frequency combs[2,3,4]

[1] S. E. Jamali Mahabadi et al., Opt. Express **27**, 3717–3730 (2019).
[2] S. E. Jamali Mahabadi et al., Opt. Lett. **46**, 813–816 (2021).
[3] S. E. Jamali Mahabadi et al., Opt. Express **29**, 11520–11532 (2021).
[4] S. E. Jamali Mahabadi et al., IEEE Photon. J. DOI: 10.1109/JPHOT.2021.3091039.

UMBC

Table of contents

UMBC

Structure of a *p*-*i*-*n* PD

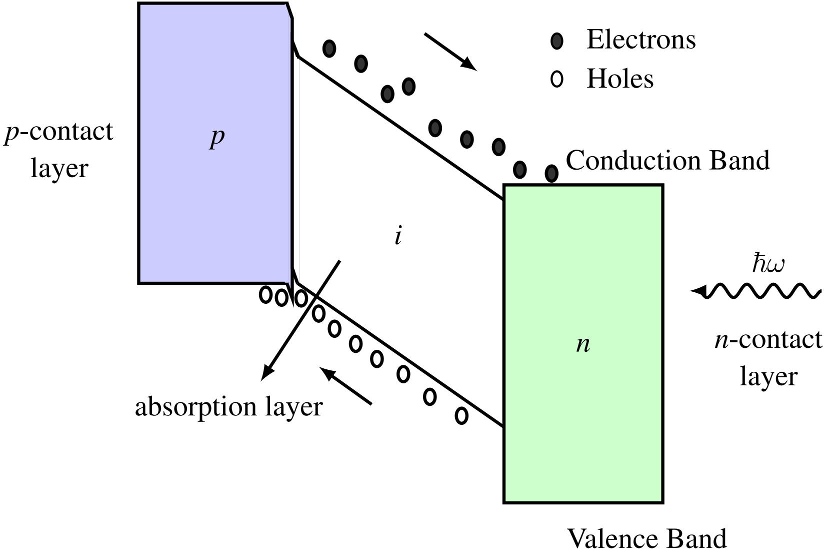

Structure of the p-i-n PD we model

Device is composed of[1]

- n-InP substrate ($N_D = 2 \times 10^{17}$ cm^{-3})
- n-InGaAs i-layer ($N_B = 5 \times 10^{15}$ cm^{-3})
- p-InGaAs p-layer ($N_A = 7 \times 10^{18}$ cm^{-3})

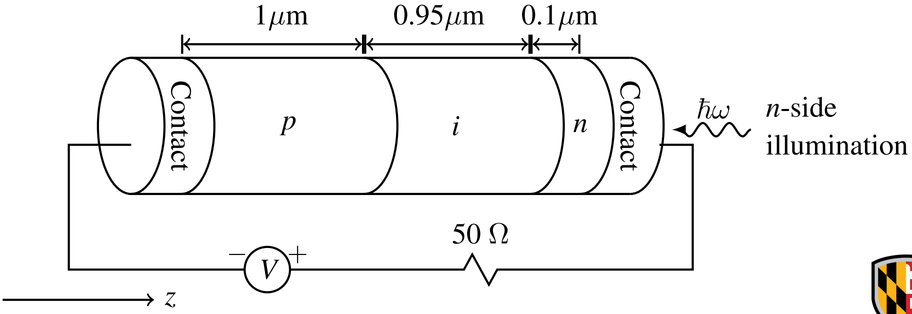

[1] K. J. Williams et al., J. Lightw. Technol. **14**, 84–96 (1996).

Structure of the *p*-*i*-*n* PD we model

Device is composed of[1]

- n-InP substrate ($N_D = 2 \times 10^{17}$ cm^{-3})
- n-InGaAs i-layer ($N_B = 5 \times 10^{15}$ cm^{-3})
- p-InGaAs p-layer ($N_A = 7 \times 10^{18}$ cm^{-3})

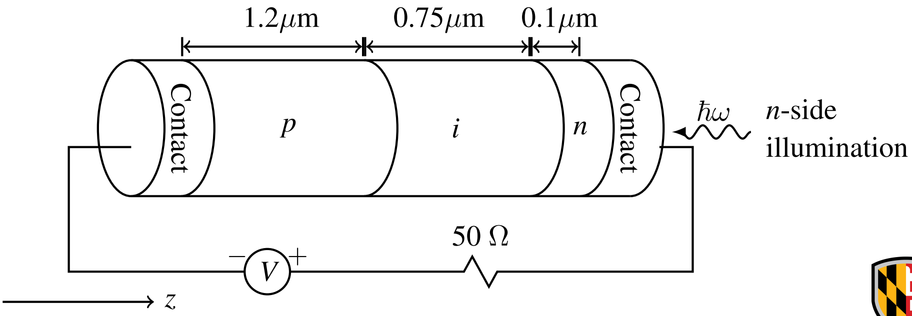

[1] K. J. Williams et al., J. Lightw. Technol. **14**, 84–96 (1996).

UMBC

Structure of a UTC PD

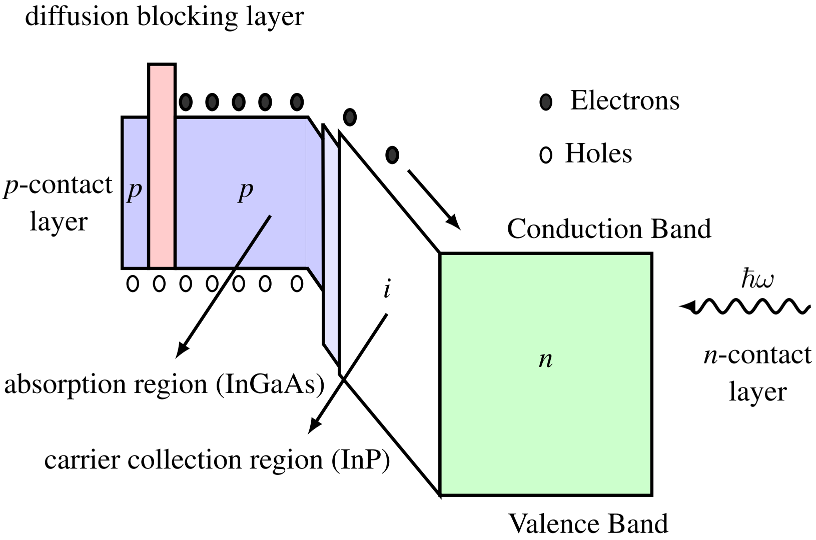

Structure of a UTC PD

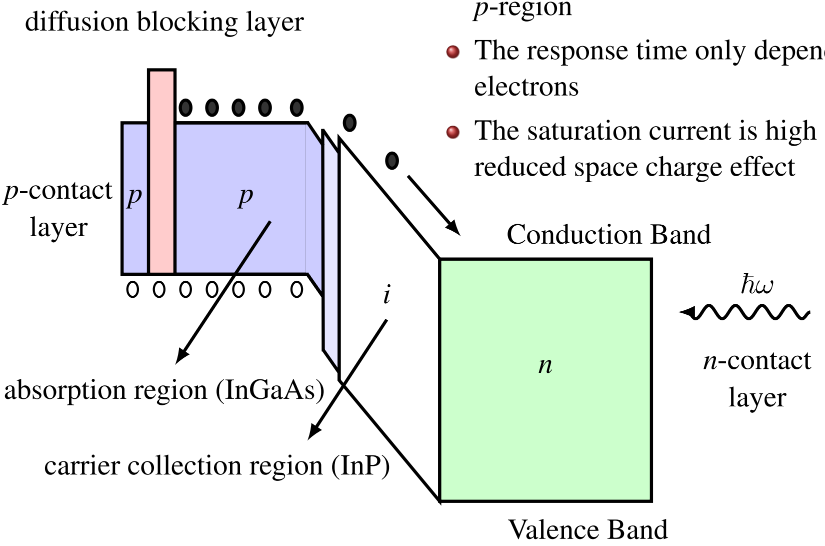

- The photons are only absorbed in the *p*-region
- The response time only depends on the electrons
- The saturation current is high due to a reduced space charge effect

UMBC

Structure of an MUTC PD

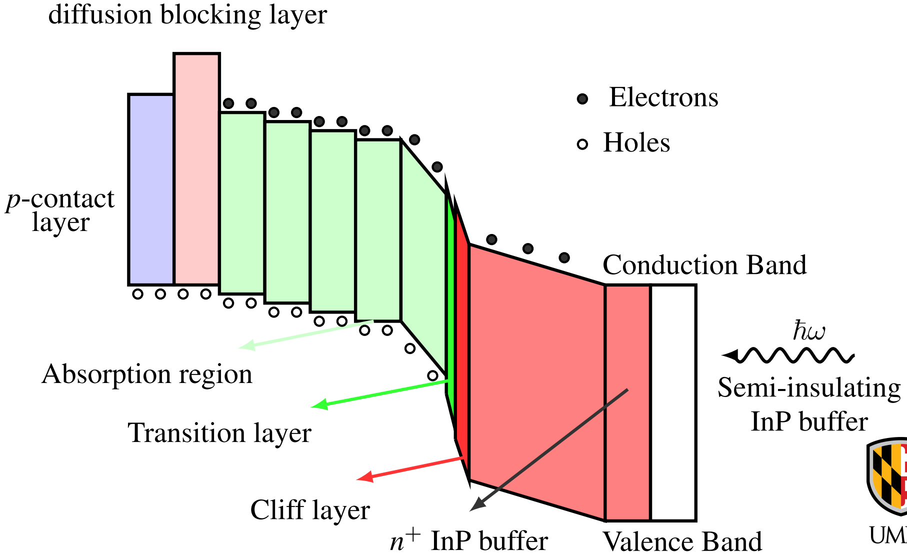

Structure of an MUTC PD

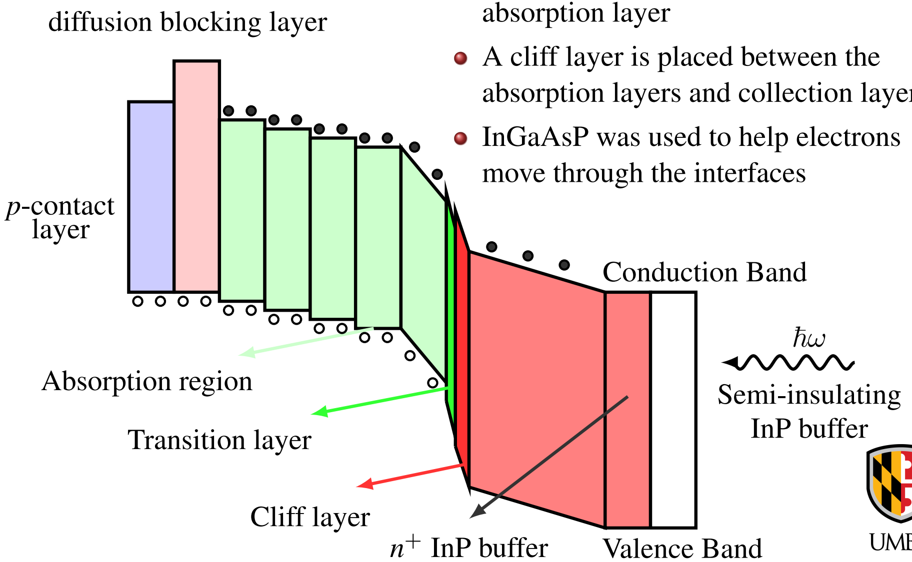

- A thin intrinsic layer was used as an absorption layer
- A cliff layer is placed between the absorption layers and collection layers
- InGaAsP was used to help electrons move through the interfaces

UMBC

Structure of the MUTC PD we model

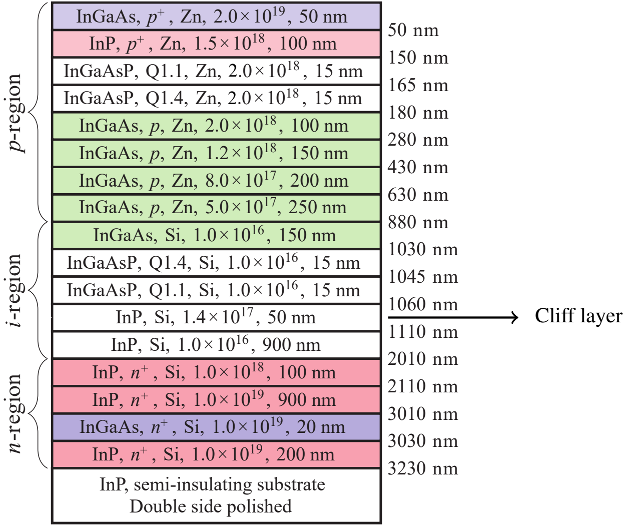

MUTC structure fabricated by Li *et al.*[1]

[1] Z. Li et al., IEEE J. Quantum Electron. **46**, 626–632 (2010).

Drift-Diffusion Model

$$\begin{aligned}\frac{\partial n}{\partial t} &= G_{\text{opt}} + G_{\text{ii}} - R(n,p) + \frac{\nabla \cdot \mathbf{J}_n}{q},\\ \frac{\partial p}{\partial t} &= G_{\text{opt}} + G_{\text{ii}} - R(n,p) - \frac{\nabla \cdot \mathbf{J}_p}{q},\\ 0 &= \nabla \cdot \nabla\varphi + \frac{q}{\epsilon}\left(N_D^+ + p - n - N_A^-\right),\end{aligned}$$

n	electron density,	p	hole density,
G_{opt}	optical generation rate,	G_{ii}	impact ionization generation rate,
R	recombination rate,	φ	electric potential,
$\mathbf{J}_n$	electron current density,	$\mathbf{J}_p$	hole current density,
N_D^+	donor density,	N_A^-	acceptor density,

UMBC

Drift-Diffusion Model

$$\mathbf{J}_p = qp\mathbf{v}_p(\mathbf{E}) - qD_p(\mathbf{E})\nabla p, \quad \mathbf{J}_n = qn\mathbf{v}_n(\mathbf{E}) + qD_n(\mathbf{E})\nabla n,$$

$$G_{\text{ii}} = \alpha_n \frac{|\mathbf{J}_n|}{q} + \alpha_p \frac{|\mathbf{J}_p|}{q}, \qquad G_{\text{opt}} = G_c \exp\left[-\alpha(L-x)\right],$$

$$G_c = Q\alpha, \qquad Q = \frac{P}{A},$$

$\mathbf{v}_n$	electron drift velocity,	$\mathbf{v}_p$	hole drift velocity,
D_n	electron diffusion coefficient,	D_p	hole diffusion coefficient,
G_c	generation rate coefficient,	α	absorption coefficient,
L	device length,	x	distance across the device,
A	the area of the light beam,	P	the power of the light beam,
α_n	electron impact ionization coefficient,	α_p	hole impact ionization coefficient,

UMBC

Velocity model

Empirical expressions that have been used to fit $\mathbf{v}_n(\mathbf{E})$ for electrons[1] and $\mathbf{v}_p(\mathbf{E})$ for the holes[2] are given by

$$\mathbf{v}_n(\mathbf{E}) = \frac{\mathbf{E}\left(\mu_n + v_{n,\text{sat}}\beta|\mathbf{E}|\right)}{1+\beta|\mathbf{E}|^2}, \quad \mathbf{v}_p(\mathbf{E}) = \frac{\mu_p v_{p,\text{sat}}\mathbf{E}}{\left(v_{p,\text{sat}}^{\gamma} + \mu_p^{\gamma}|\mathbf{E}|^{\gamma}\right)^{1/\gamma}},$$

μ_n	:	low-field electron mobility,	μ_p	:	low-field hole mobility,
$v_{n,\text{sat}}$	:	saturated electron velocity,	$v_{p,\text{sat}}$	:	saturated hole velocity,
β	:	fitting parameter,	γ	:	fitting parameter,

[1] M. Dentan and B. de Cremoux, J. Lightw. Technol. **8**, 1137–1144 (1990).

[2] K. W. Böer, *Survey of Semiconductor Physics* (Van Nostrand Reinhold, 1990).

UMBC

Velocity of electrons and holes in InGaAs

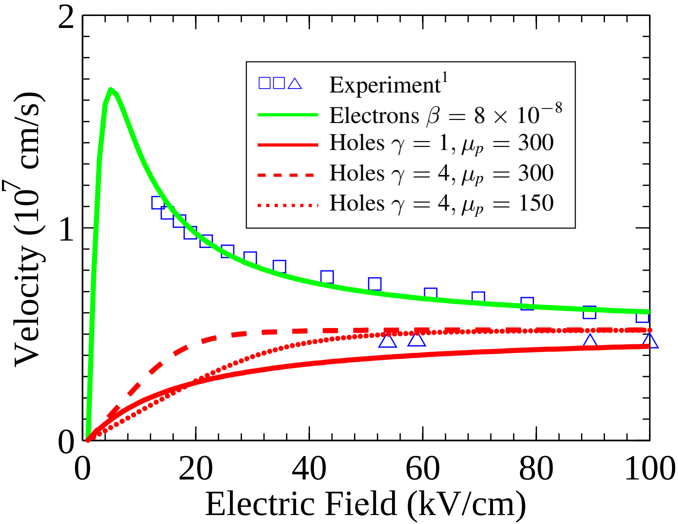

[1] T. H. Windhorn et al., J Electron. Mater. **11**, 1065–1082 (1982).

UMBC

Diffusion model

Empirical expressions that have been used to fit $D_n(\mathbf{E})$ for electrons[1] and $D_p(\mathbf{E})$ for the holes[2] are given by

$$D_n(\mathbf{E}) = \frac{k_B T \mu_n / q}{\left[1 - 2\left(|\mathbf{E}|/E_p\right)^2 + \frac{4}{3}\left(|\mathbf{E}|/E_p\right)^3\right]^{1/4}}, \quad D_p(\mathbf{E}) = \frac{k_B T}{q}\frac{\mathbf{v}_p(\mathbf{E})}{\mathbf{E}},$$

E_p : fitting parameter, 4×10^3 V/cm

[1] K. W. Böer, *Survey of Semiconductor Physics* (Van Nostrand Reinhold, 1990).
[2] K. J. Williams, "Microwave nonlinearities in photodiodes," PhD Dissertation, University of Maryland College Park, Maryland, USA, 1994.

UMBC

Diffusion model

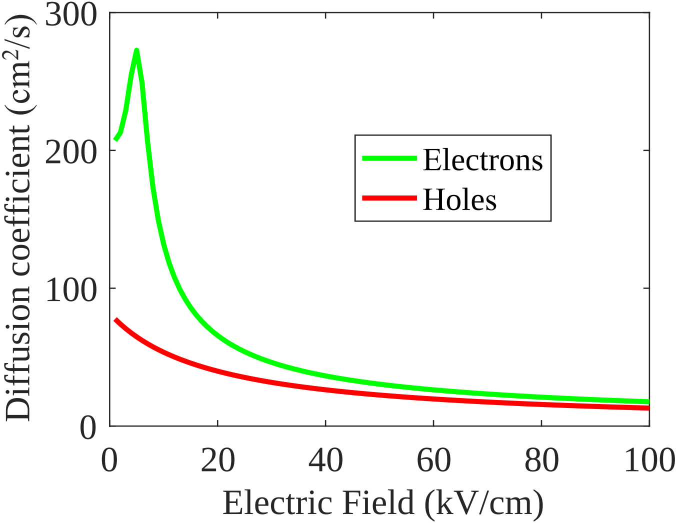

UMBC

Drift-diffusion coefficients

- The electron velocity and diffusion decrease when the field increases
- Why?
  - electrons transition from the Γ-valley to the L-valley and X-valley
  - their effective mass increases[1]

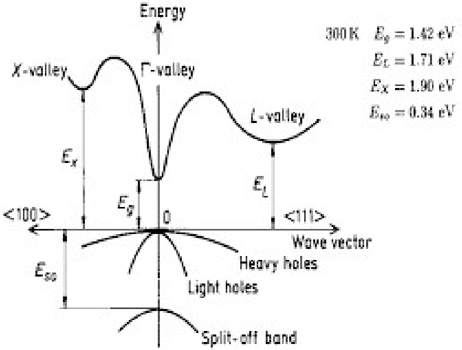

[1] Y. A. Goldberg and N. M. Schmidt, *Handbook Series on Semiconductor Parameters* (World Scientific, London, 1999).

Recombination-Generation

- The largest contribution to recombination is the Shockley-Read-Hall (SRH) effect.
  - also known as trap-assisted nonradiative recombination
  - the expression for SRH recombination is

$$R = \frac{np - n_i^2}{\tau_p(n + n_i) + \tau_n(p + n_i)},$$

τ_n	:	electron lifetime,	τ_p	:	hole lifetime,
n_i	:	intrinsic doping concentration,			

- The generation rate from impact ionization:

$$G_{\mathrm{ii}} = \alpha_n \frac{|\mathbf{J}_n|}{q} + \alpha_p \frac{|\mathbf{J}_p|}{q}, \ \alpha_{n,p} = A_{n,p} \cdot \exp\left[- \left(\frac{B_{n,p}}{|\mathbf{E}|} \right)^m \right],$$

A_n, A_p, B_n, B_p, m : impact ionization parameters

UMBC

Implicit method

Fully implicit method[1] (backwards Euler method) is used to solve the equations

$$\begin{aligned}
\frac{n^{t+1} - n^t}{\Delta t} &= F_n(n^{t+1}, p^{t+1}, \varphi^{t+1}) \\
\frac{p^{t+1} - p^t}{\Delta t} &= F_p(n^{t+1}, p^{t+1}, \varphi^{t+1}) \\
0 &= F_\varphi(n^{t+1}, p^{t+1}, \varphi^{t+1})
\end{aligned}$$

[1] S. Selberherr, *Analysis and simulation of semiconductor devices* (Springer-Verlag Wien, 1984).

UMBC

Modeling Approach (1-D Scheme)

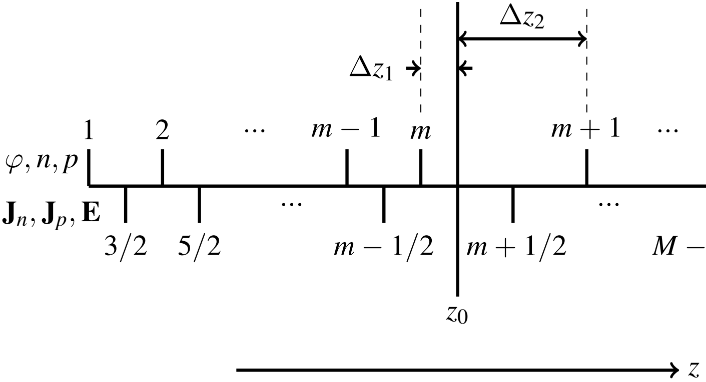

Gridding scheme used in device model for multilayer devices

- φ, n, p are defined at integer grid values
- $\mathbf{J}_n, \mathbf{J}_p, \mathbf{E}$ are defined at half-integer grid values

UMBC

1-D model: light beam

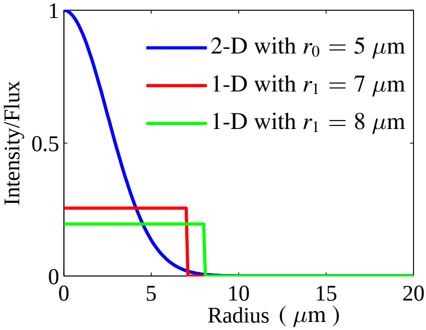

- In 2-D simulations, we assume that the beam is Gaussian-shaped with a profile given by

$$Q(r,t) = Q_0(t)\exp\left[-2\,(r/r_0)^2\right],$$

- In 1-D simulations, the physical Gaussian beam profile must be approximated by a constant intensity Q_{1d} over an effective beam area with r_1, so that

$$\int_0^\infty 2\pi r Q(r,t)dr = \pi r_1^2 Q_{1d}$$

UMBC

Table of contents

UMBC

Harmonic powers in CW mode

Simulation results: 1-D vs. 2-D

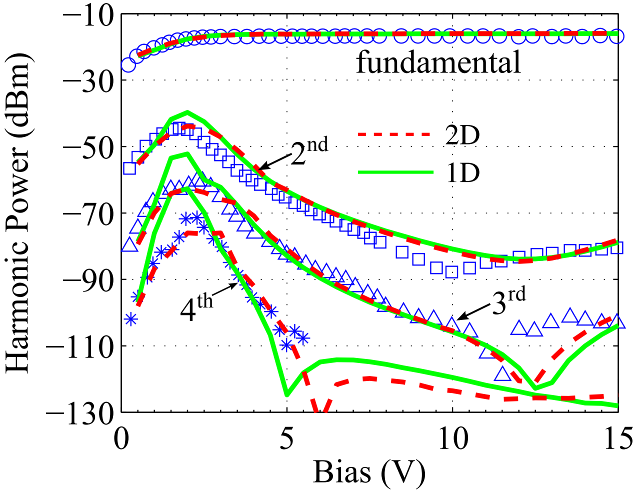

Impact ionization

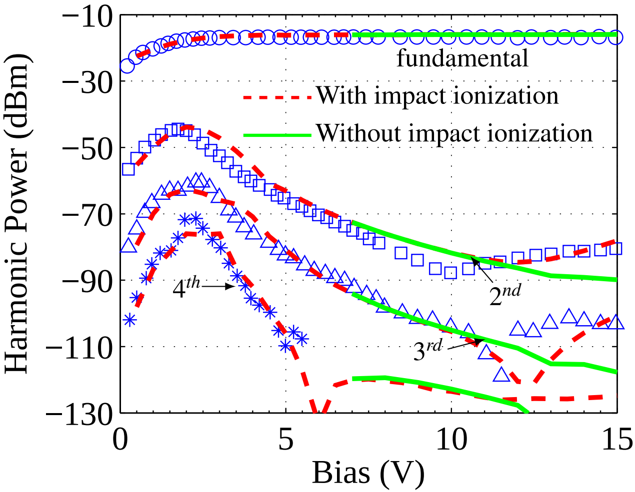

Summary for the *p-i-n* PD

- We studied 1-D and 2-D models of a single heterojunction *p-i-n* PD that are based on the drift-diffusion equations.
- We obtained excellent agreement with experiments
- We have examined the impact of
  - An external load
  - Thermionic emission
  - Impact ionization

Conclusion

The dominant physical cause of the observed saturation and the increased nonlinearity at large reverse bias is impact ionization

[1] Y. Hu, et al., J Lightw. Tech. **32**, 3710–3720 (2014).

UMBC

Table of contents

UMBC

Frequency combs

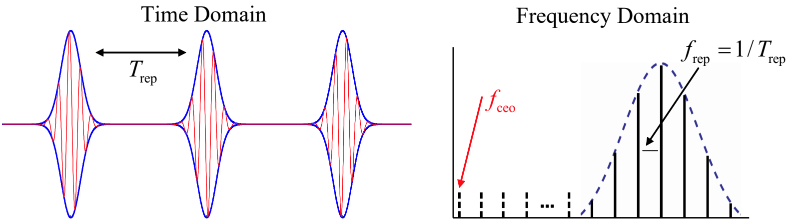

Microwave generation

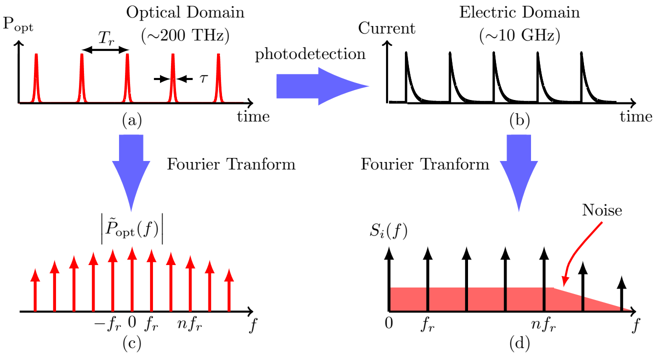

Remark

Optical amplitude noise can be converted into phase noise. We will analyze amplitude-to-phase noise conversion in the PD

[1] T. M. Fortier et al., Opt. Lett. **38**, 1712–1714 (2013).

UMBC

AM-to-PM

- The amplitude-to-phase noise coefficient $\alpha_{\mathrm{AM/PM}}$ can be defined as the induced root mean square phase variation arising from a fractional power change

$$\alpha_{\mathrm{AM/PM}} = \left| \frac{\Delta\phi}{\Delta P/P} \right|,$$

$\Delta P/P$	:	fractional power change
$\Delta\phi$	:	phase change

- One method to measure AM-to-PM conversion is to measure the time-domain impulse response of the PD and to use a Fourier transform to calculate the phase difference as the power varies

[1] J. Taylor et al., IEEE Photonics J. **3**, 140–151 (2011).

UMBC

Experimental results

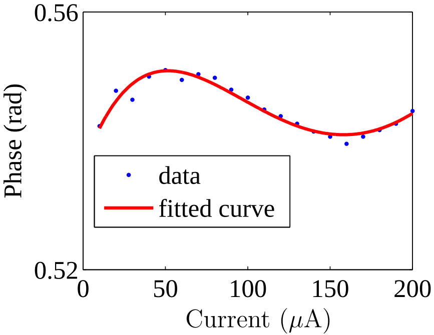

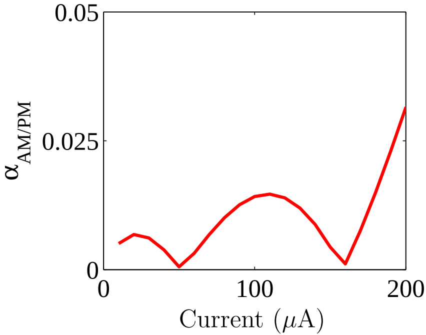

- There are two null points
- At these two points, the AM-to-PM noise conversion is zero
- What is physical reason?

[1] J. Taylor et al., IEEE Photonics J. **3**, 140–151 (2011).

UMBC

Simulation results

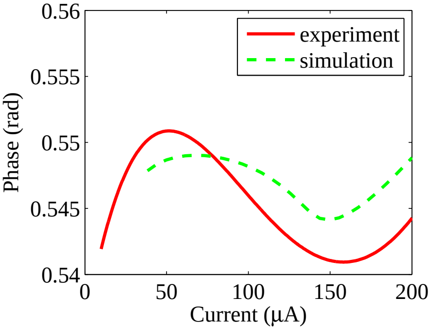

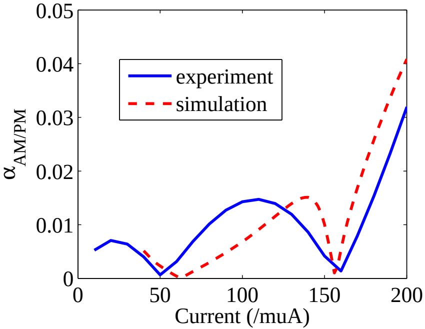

- We obtain good agreement with experimental results for the location of nulls

UMBC

Summary of AM to PM conversion

- The appearance of nulls in the AM-to-PM noise conversion is due to the nonlinear dependence of the electron velocity on the electric field
- When the pulse duration is reduced below 500 fs, the AM-to-PM noise conversion coefficient does not change
- When the pulse duration is greater than 500 fs, the second null in the AM-to-PM shifts to larger photocurrents
- The repetition rate does not change the AM-to-PM conversion coefficient
- The AM-to-PM noise conversion coefficient can be greatly reduced by removing InGaAs and InP heterojunction

UMBC

Table of contents

UMBC

Calculation of the phase noise in MUTC PDs

- The mean-square phase fluctuation is given by

$$\left\langle \Phi_n^2 \right\rangle = \frac{1}{N_{\text{tot}}} \frac{\int_0^{T_R} h(t) \sin^2\left[2\pi n(t-t_c)/T_R\right] \mathrm{d}t}{\left\{\int_0^{T_R} h(t) \cos\left[2\pi n(t-t_c)/T_R\right] \mathrm{d}t\right\}^2},$$

  - N_{tot} = total number of electrons in the photocurrent
  - t_c = central time of the output current
  - T_R = repetition time between optical pulses
- In the limit of short optical pulse widths ($\lesssim$ 500 fs):
  - $\langle \Phi_n^2 \rangle$ tends to a non-zero constant

$$\left\langle \Phi_n^2 \right\rangle = \frac{1}{N_{\text{tot}}} \frac{\int_0^{T_R} h_e(t) \sin^2\left[2\pi n(t-t_c)/T_R\right] \mathrm{d}t}{\left\{\int_0^{T_R} h_e(t) \cos\left[2\pi n(t-t_c)/T_R\right] \mathrm{d}t\right\}^2},$$

    - ★ $h_e(t)$ = electronic impulse response of the device

UMBC

Phase noise results

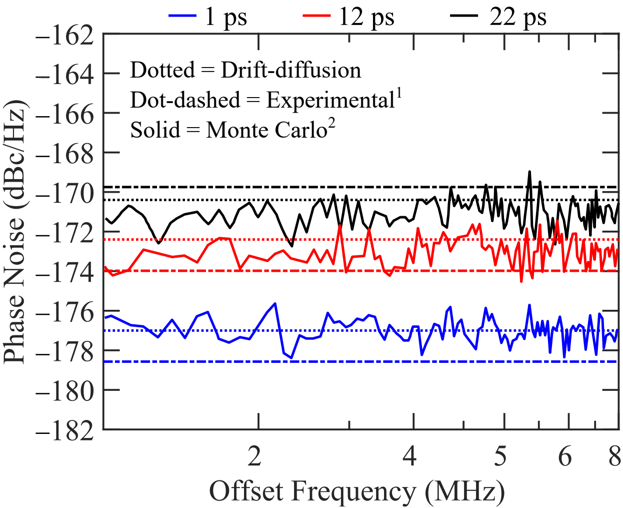

[1] F. Quinlan et al., Nat. Photonics **7**, 290–293 (2013).
[2] W. Sun et al., Phys. Rev. Lett. **113**, 203901 (2014).

Phase noise results

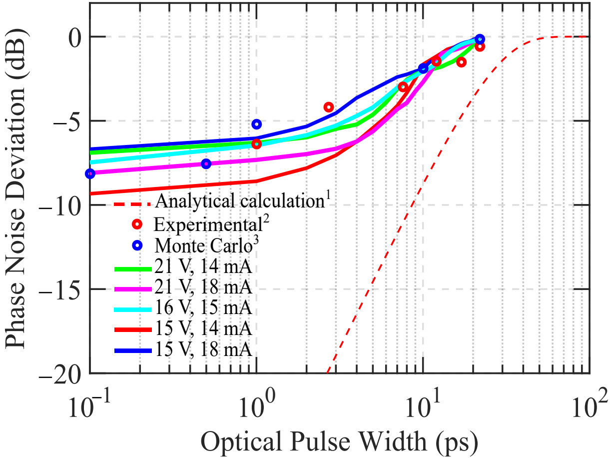

[1] F. Quinlan et al., J. Opt. Soc. Am. B **30**, 1775–1785 (2013).

[2] F. Quinlan et al., Nat. Photonics **7**, 290–293 (2013).

[3] W. Sun et al., Phys. Rev. Lett. **113**, 203901 (2014).

UMBC

Device optimization

- Our goal is to reduce the tails in the impulse response
  - A long tail in the impulse response translates to higher phase noise
- We first altered the thickness of each absorption layer up to 10%
  - no significant change
- We next altered the doping density in each of the absorption layers
  - we obtained an impulse response with a smaller tail to lower the phase noise

UMBC

Device optimization

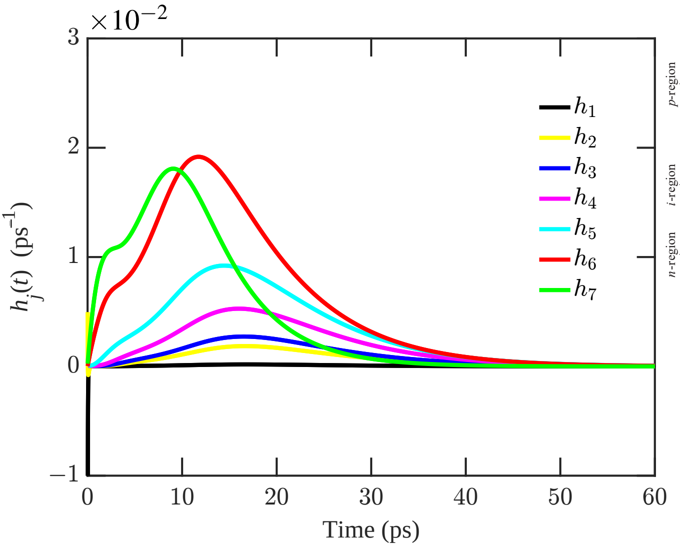

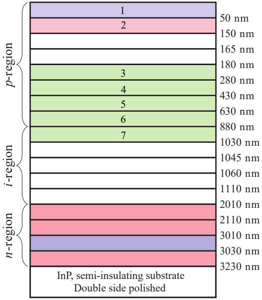

$$h(t) = \sum_{j=1}^{N} h_j(t),$$

UMBC

Device optimization

- Phase Noise 1 = phase noise of the Li et al.[1] structure
- Phase Noise 2 = phase noise of the modified structure
- Difference = (Phase Noise 1) − (Phase Noise 2)

Pulse Width	Original structure	Modified structure	Difference
1 ps	−178.6 dBc/Hz	−180.0 dBc/Hz	1.4 dBc/Hz
12 ps	−174.0 dBc/Hz	−175.5 dBc/Hz	1.5 dBc/Hz
22 ps	−169.7 dBc/Hz	−172.8 dBc/Hz	3.1 dBc/Hz

[1] Z. Li et al., IEEE J. Quantum Electron. **46**, 626–632 (2010).

UMBC

Summary of phase noise

- We used the drift-diffusion equations to calculate
  - the impulse response
  - the phase noise

  in an MUTC PD with short optical pulses
- We found excellent agreement with prior experiments[1] and Monte Carlo simulations[2]
- Optimization results:
  - we designed a structure with
    - lower phase noise
    - reduced nonlinearity

[1] F. Quinlan et al., Nat. Photonics **7**, 290–293 (2013).
[2] W. Sun et al., Phys. Rev. Lett. **113**, 203901 (2014).

UMBC

Table of contents

UMBC

Characterization of nonlinearity

Measurement setup[1]

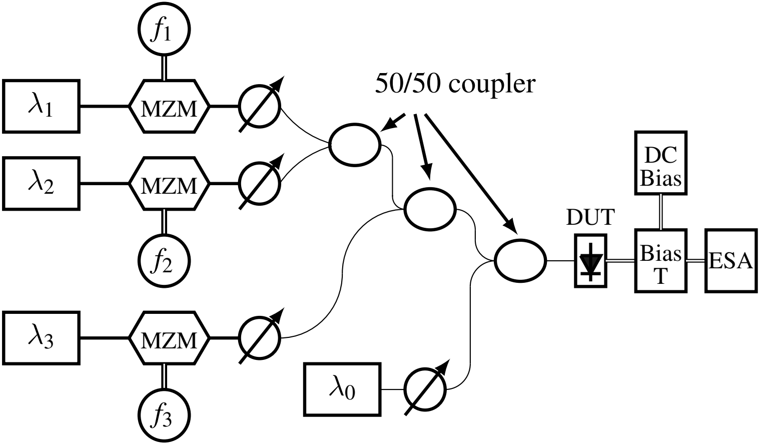

[1] M. Draa et al., Opt. Express **19**, 12635-12645 (2011).

Characterization of nonlinearity

The input modulated average light power $P(t)$:

$$P(t) = P_0(t)\left\{1 + m\left[\sin\left(2\pi f_1 t\right) + \sin\left(2\pi f_2 t\right) + \sin\left(2\pi f_3 t\right)\right]\right\},$$

- In the CW mode
  - $P_0(t)$ is a constant value as a function of time
- In the pulsed mode
  - $P_0(t)$ is given by

$$P_0(t) = \sum_n A_0 \operatorname{sech}\left(\frac{t - nT_r}{\tau}\right),$$

$P_0(t)$	:	input average light power	t	:	time
m	:	modulation depth	τ	:	pulse width
f_1, f_2, and f_3	:	three modulation frequencies	T_r	:	repetition time

UMBC

Characterization of nonlinearity

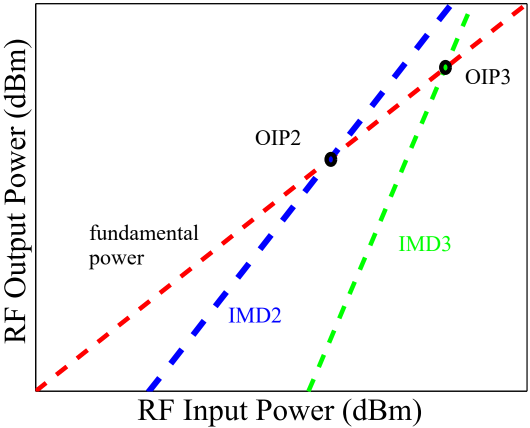

$$\mathrm{OIP3} = P_f + \frac{1}{2}\left(P_f - P_{\mathrm{IMD3}}\right)\ (\mathrm{dBm}),$$
$$\mathrm{OIP2} = 2P_f - P_{\mathrm{IMD2}}\ (\mathrm{dBm}),$$

UMBC

Spectrum of a CW three-tone modulated input

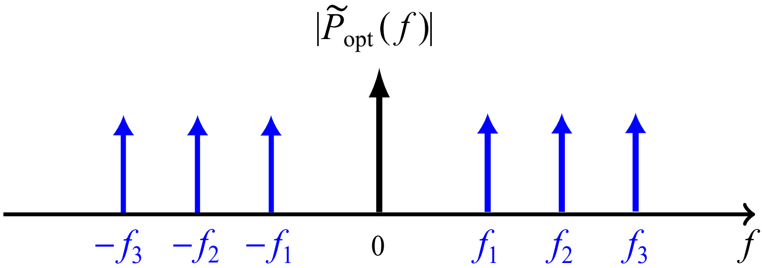

$\widetilde{P}_{\mathrm{opt}}(f)$ is the Fourier transform of $P_{\mathrm{opt}}(t)$

$$P_{\mathrm{opt}}(t) = P_0(t)\left\{1 + m\left[\sin\left(2\pi f_1 t\right) + \sin\left(2\pi f_2 t\right) + \sin\left(2\pi f_3 t\right)\right]\right\},$$

UMBC

Comb generation with a pulsed input

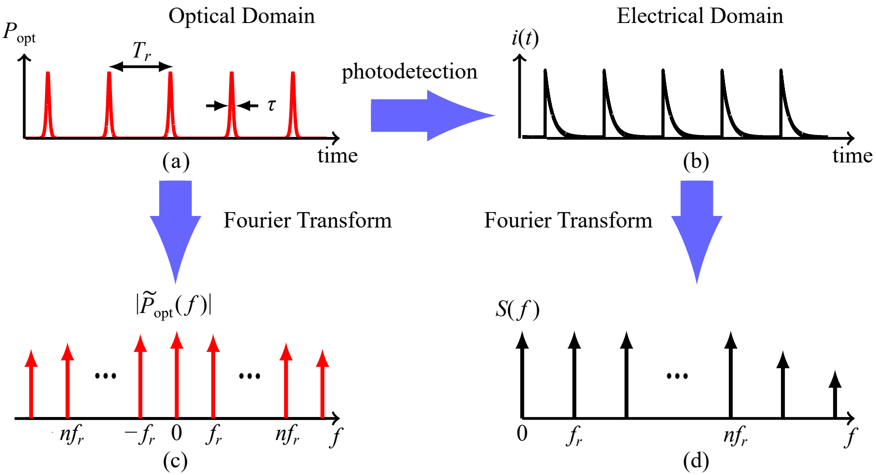

$$P_{opt}(t) = \sum_n A_0 \operatorname{sech}\left(\frac{t - nT_r}{\tau}\right),$$

UMBC

Comb generation with an RF-modulated input

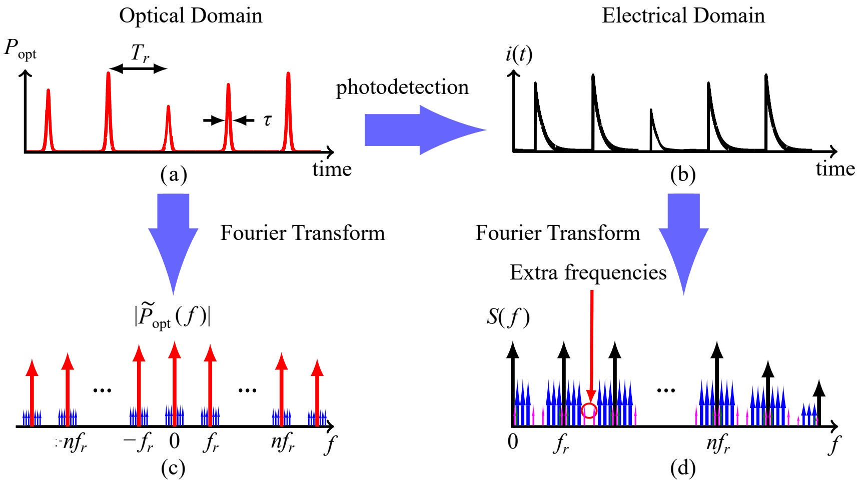

$$P_{opt}(t) = P_0(t)\left\{1 + m\left[\sin\left(2\pi f_1 t\right) + \sin\left(2\pi f_2 t\right) + \sin\left(2\pi f_3 t\right)\right]\right\},$$

$$P_0(t) = \sum_n A_0 \operatorname{sech}\left(\frac{t - nT_r}{\tau}\right),$$

UMBC

Comb generation with an RF-modulated input

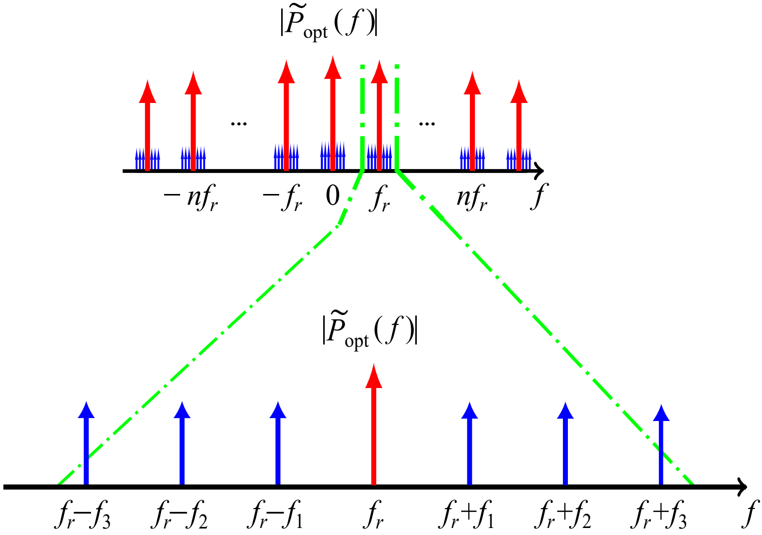

UMBC

Comb generation with an RF-modulated input

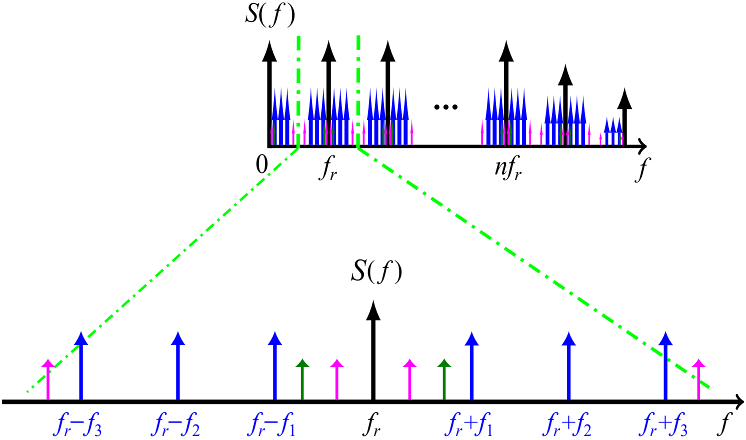

UMBC

Comb generation with an RF-modulated input

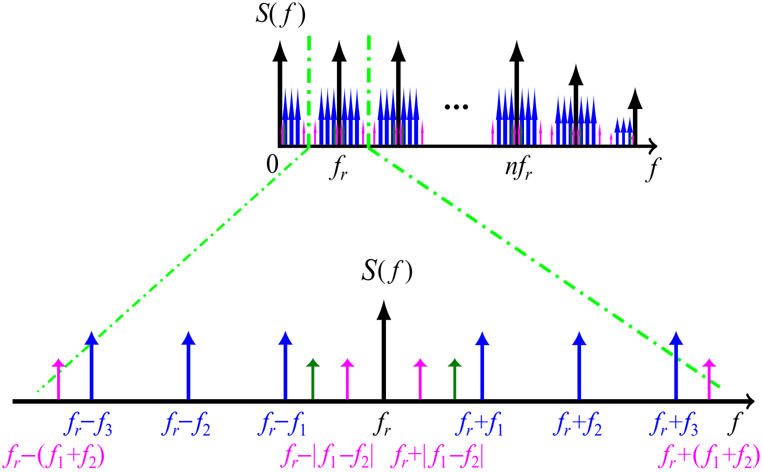

UMBC

Comb generation with an RF-modulated input

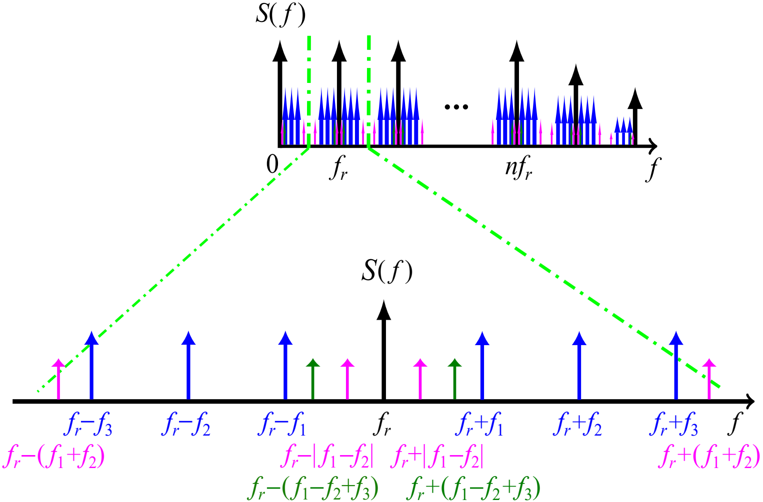

UMBC

Nonlinearity characterization: CW vs. pulsed mode

- For CW mode
  - there is only one IMD2 and one IMD3
  - there is only one OIP2 and one OIP3
- **For pulsed mode**
  - **there is one IMD2_n and one IMD3_n for each comb line n**
  - **there is one OIP2_n and one OIP3_n for each comb line n**

CW		Pulsed
IMD2	→	IMD2_n
IMD3	→	IMD3_n
OIP2	→	OIP2_n
OIP3	→	OIP3_n

Subscript n indicates the comb line number

UMBC

Bleaching in PDs

Empirical Bleaching Model

In the drift diffusion equations:

$$G_{\text{opt}} = B_f \, G_c \exp\left[-\alpha(L - x)\right],$$

$$B_f = \frac{A + BI_{\text{p}}}{C + DI_{\text{p}} + EI_{\text{p}}^2},$$

Fitting parameters	p-i-n	MUTC
A	1.0000	1.0000
B	0.0098	0.0322
C	0.6526	2.7181
D	0.0236	0.1632
E	0.0015	0.0016

UMBC

Experimental and empirical results

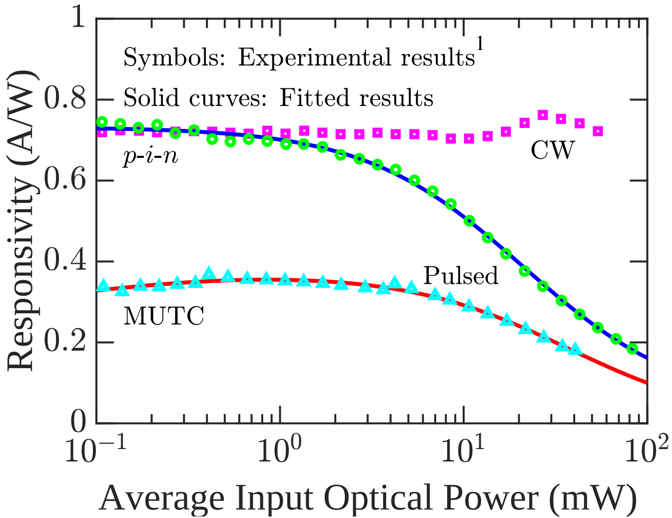

[1] S. E. Jamali Mahabadi et al., Opt. Lett. **46**, 813–816 (2021).

UMBC

Characterization of nonlinearity

- We calculated the impact of the bleaching on the device nonlinearity as a function of the average optical power
- We calculated the second- and third-order intermodulation distortion (IMD2 and IMD3) powers
  - frequencies that IMD3 generates can introduce spurious signals
    - that cannot be filtered out from the fundamental response
    - this is important for microwave photonic applications where these would appear as false signals of interest
- We calculated the second- and third-order output intercept points (OIP2 and OIP3) to characterize IMD2 and IMD3

UMBC

OIP2$_n$ and OIP3$_n$ in the MUTC PD

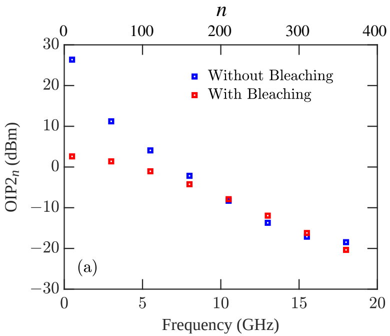

- OIPs decrease as frequency increases with and without bleaching
- OIPs are bigger at low frequencies without bleaching
- The effect of bleaching vanishes between 10 GHz and 16 GHz
  - due to decrease in space charge
- It reappears beyond 16 GHz
  - due to reduction in powers

UMBC

OIP2$_n$ and OIP3$_n$ in the p-i-n PD

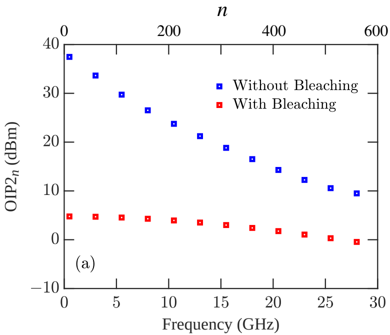

- OIPs decrease as frequency increases without bleaching
- They are almost flat with bleaching
  - the decrease in space charge compensates for the decrease in responsivity
- The gap decreases as frequency increases

UMBC

Distortion-to-signal ratios

We define distortion-to-signal as

$$\rho_{2n} = \mathrm{IMD2}_n / S_n, \qquad \rho_{3n} = \mathrm{IMD3}_n / S_n,$$

Comparison of ρ_{2n} and ρ_{3n}

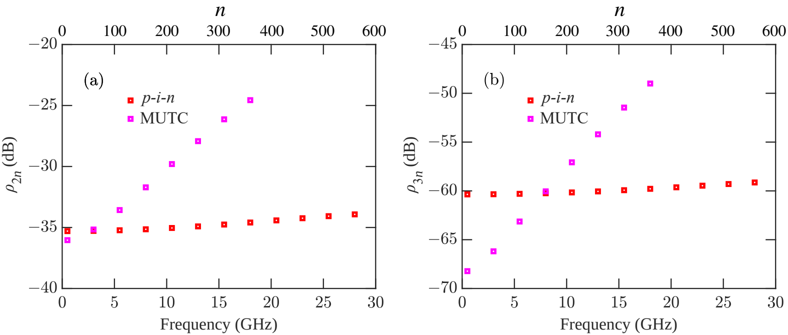

- The ratios increase rapidly for the MUTC PD
- The ratios remain relatively flat for the *p-i-n* PD

UMBC

Comparison of ρ_{2n} and ρ_{3n}

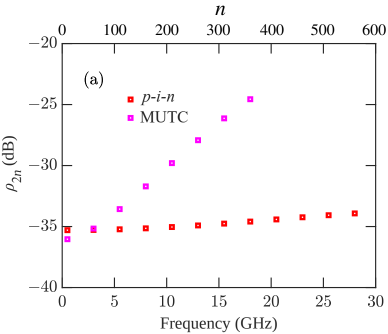

- *p-i-n* PD has better performance at high frequencies
  - this is surprising
    - it is well known that MUTC PDs have less distortion in CW
- MUTC PD has better performance at low frequencies

UMBC

Comparison of ρ_{2n} and ρ_{3n}

Why does nonlinearity have more impact on the MUTCs at high frequencies?

- Distortion products are summed contributions from many comb lines
  - distortion product at $nf_r + (f_1 - f_2)$ is obtained from: signals at $lf_r + f_1$ and $mf_r - f_2$ with $l + m = n$ for all l and m
- The distortion products add more coherently in the MUTC PD than they do in the *p-i-n* PD
  - MUTC PD
    - the current in the MUTC PD is almost entirely due to electrons
  - *p-i-n* PD
    - the current has significant contributions from both electrons and holes
    - we attribute the lower coherence of the distortion products at each frequency to the presence of two carriers

UMBC

Summary of nonlinearity in frequency combs with bleaching

- We have developed an empirical model of bleaching
  - we determined the parameters of bleaching model
  - we obtained good agreement with experimental results
- We calculated IMD2$_n$ and IMD3$_n$ in the *p-i-n* and MUTC PDs
  - taking into account bleaching
  - **Note: There is a separate IMD2$_n$ and IMD3$_n$ for each comb-line where n is the comb line number**
- We calculated OIP2$_n$ and OIP3$_n$ to characterize IMD2$_n$ and IMD3$_n$ for each comb line n
- We calculated distortion-to-noise ratios ρ_{2n} and ρ_{3n}

Summary of nonlinearity in frequency combs with bleaching

- The principal effect of bleaching is to lower the responsivity
  - decreases the number of electrons in the device
    - ★ lowers the nonlinearity due to space-charge effects
  - the decrease becomes more pronounced as input optical power increases
    - ★ fundamental comb powers S_n and the intermodulation products saturate
  - the impact of bleaching decreases at high comb line numbers
- The difference in behavior of ρ_{2n} and ρ_{3n} between the *p-i-n* PD and MUTC PD is due to
  - greater coherence of the nonlinear products in the MUTC PD
  - the impact in the MUTC PD increases at high comb line numbers

UMBC

Table of contents

UMBC

Future Initiative: Intelligent optimization (E. Simsek)

Machine Learning: Prediction Using an Artificial Neural Network (ANN)

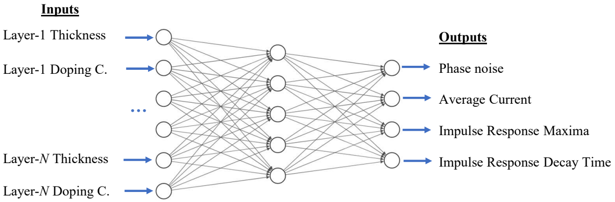

Preliminary Results

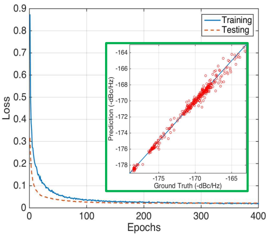

	Performance Metric Statistics			Prediction Errors (%)			
	Minimum	Maximum	CV	LR	kNN	RF	ANN
Phase noise	-178.62 dBc/Hz	-161.51 dBc/Hz	-0.022	0.38	0.39	0.19	0.18
Ave. Current	1.46 mA	9.9 mA	0.65	16.81	5.16	3.5	2.47
IR Max	28.5 ns^{-1}	97.56 ns^{-1}	0.22	4.81	5.48	3.06	2.88
Decay Time	22.22 ns	184.77 ns	0.5	9.91	11.34	7.12	5.21

UMBC

Future Initiative: Intelligent optimization (E. Simsek)

Machine Learning: Design

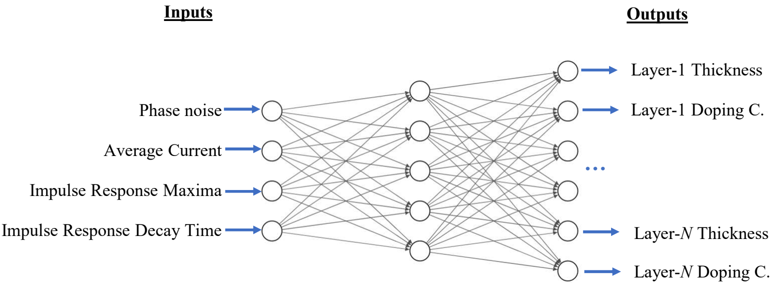

Preliminary Results: The design, recommended by an ANN trained with 1000+ samples, outperforms all PDs used in training.

UMBC

Thank you for your attention